Experimental and Finite Element Investigation of Composite Beams Consisting of Reinforced Concrete Prisms Cast Into Steel Channels

Laith Khalid Al-Hadithy
Nahrain University/College of Engineering.
E-mail:lthadithy@yahoo.com

Omer Khalid Al-Kerbooli
Nahrain University/College of Engineering.
E-mail:omerkhalid79@yahoo.com

Abstract

Four reinforced concrete beams of rectangular cross-sections and four corresponding composite ones consisting of reinforced concrete prisms cast into steel channels with shear connectors were manufactured, loaded, and tested in the laboratory to measure mid-span deflections, and to observe fracture criteria. The reinforced concrete prism of each of the four composite beams is of rectangular cross-section and identical to its corresponding reinforced concrete beam.

Load-deflection behavior and fracture pattern at failure obtained experimentally for each of the eight beams were compared with those predicted by a nonlinear three-dimensional finite element analysis using the analysis system computer program (ANSYS V. 5.4) in which the reinforced concrete, the steel channel, and the interaction between reinforced concrete and steel channel were modeled by isoparametric eight-node brick elements, four-node shell elements ,and the five-node interface elements ,respectively.

High agreement between the experimental tests and the numerical models was obtained for load-deflection behavior represented by maximum differences of 11% and 7% for composite and non-composite beams, respectively. In addition, a perfect coincidence in predicting fracture pattern at failure by the two methods was realized.

Comparisons between flexural behaviors for each of the present four pairs of correspondent composite and non-composite beams show that introducing the integrated steel channels highly increases the ultimate load capacity by 155% to 500% -depending on the ratio of steel channel area to gross concrete area, and decreases the ductility ratio by 26.4% to 36.7% -depending on the ratio of steel channel area to tension reinforcement area.

A parametric study on the effect of flange width of the steel channel show that a 40% increase in the ultimate load capacity can be realized by a one-third increase in that parameter with a slight decrease in ductility ratio.

1. Introduction

Composite beams consisting of reinforced concrete prisms of rectangular cross-sections (forming the dominant part of the whole cross-sections) cast into steel channels, as shown in Fig.1 provide good economy because the expensive material which is represented by the steel channel is used in greater benefit. The steel channel is placed at the bottom of the cross-section providing greater lever arm between the two centers of compression and tension forces.

Structural behavior of the present beam depends mainly on the composite action represented by the flexural stiffness of the steel channel supporting the overhead rectangular reinforced concrete beam, with the structural integrity created by the shear connectors that enable the whole composite section to support all the loads.

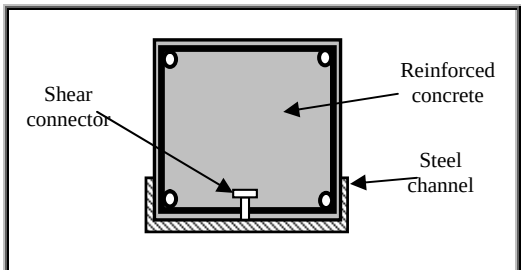

Figure (1) Composite beam consisting of a steel channel interconnected to an overhead rectangular reinforced concrete beam by shear connector.

The steel channel also provides some additional advantages. Firstly, it provides the main part of the formwork for the rectangular reinforced concrete part of the composite beam with no need to temporary shoring. Secondly, it abolishes the necessity of using tensile longitudinal reinforcing bars (with their anchorage requirements) in simply supported beams. Occasional introduction of a few small diameter bars in those locations without any anchorage requirements-depends on the need to fix transverse reinforcement (stirrups) in place.

The present steel-concrete composite system is not covered by the ACI specifications or the British Standards for structural concrete. On the other hand, application of the steel construction specifications (like the AISC specifications) to composite

construction is limited to two traditional composite cases: totally encased steel beams, and steel beams supporting concrete slabs with the use of shear connectors. That fact makes the present composite system unrestricted by any specification.

Few researches dealing with reinforced concrete beams cast into steel channels were done and none of them studied the case of rectangular reinforced concrete part. **Taylor, in 1979 [1]** made an experimental study on a variety of simply supported beams using two types of testing. **Taylor and Burdon ,in 1972 [2]** reported tests on six simply supported composite beams having the cross section shown in Fig.2 with mild steel channel as tensile reinforcement. **Taylor and Najmi ,in1980 [3]** reported tests on six simply supported composite beams having the cross section shown in Fig.3 with mild steel channels as compression reinforcement.

Yousif, in 1982 [4], made an experimental study by using four simply supported reinforced concrete T-beams cast into steel channels,Fig.2 , simulating them as parts of a continuous beam at support section, tested to investigate their behavior in shear and in hogging bending. Test data were critically analyzed to suggest the methods of prediction of shear and flexural loads, and to explore the possibilities of the application of simple plastic theory for the analysis of continuous composite reinforced concrete beams.

Abd Al-Razag, in 1985 [5], made another experimental study by using six simply supported reinforced concrete T-beams cast into steel channel, Fig.3 , to investigate the behavior of sagging moment regions. He suggested a computerized method of analysis based on the theoretical moment-curvature relationship for sagging moment section. By that program-the computerized methods- the short-term deflection at service load can be calculated based on gross concrete section, neglecting reinforcement.

The present study includes an experimental work (model manufacturing and testing) which is necessary for the assessment of the accuracy and validity of the proposed theoretical method (finite element model).

The main objective of this research is to conduct a finite-element investigation on the behavior of the composite beam consisting of a rectangular reinforced concrete part cast into a steel channel. Material nonlinearity due to cracking of concrete in tension, plastic flow or crushing of concrete in compression, yielding of steel and the interface between steel and concrete are included.

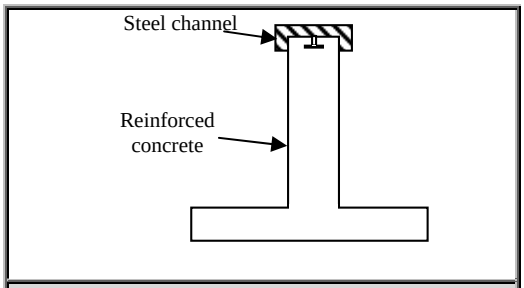

Figure (2) Cross-section of the hogging type of the T-section reinnforced concrete beam cast into steel channel [2]

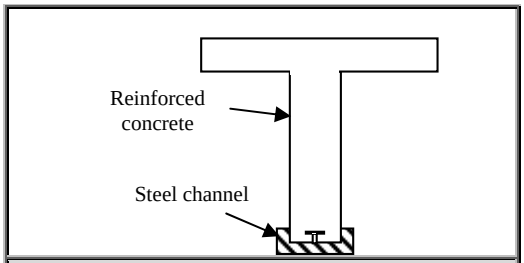

Figure (3) Cross-section of the sagging type of the T-section reinnforced concrete beam cast into steel channel [3]

2. Experimental work

2.1 Description of Test Specimens

Eight beams were fabricated, loaded and tested. All the beams were simply supported having 1200 mm spans. They were divided into two groups, each consisting of four beams. Beams of the first group, shown in Fig. 4, were non-composite reinforced concrete ones varying in cross-sectional dimensions, reinforcement and overhanging lengths. Each beam in the second group, shown in Fig. 5, consisted of a steel channel and a reinforced concrete prism similar to the corresponding rectangular reinforced concrete non-composite beam in the first group. The two parts of a composite beam are interconnected for shear and split is represented by shear studs attached to the interior face of the steel channel web by fillet welding at mid spacing of the stirrups as shown in Fig. 5. Sectional dimensions of the used steel channels were of two types; 1 and 2 as shown in Fig. 6 with details of their shear connectors.

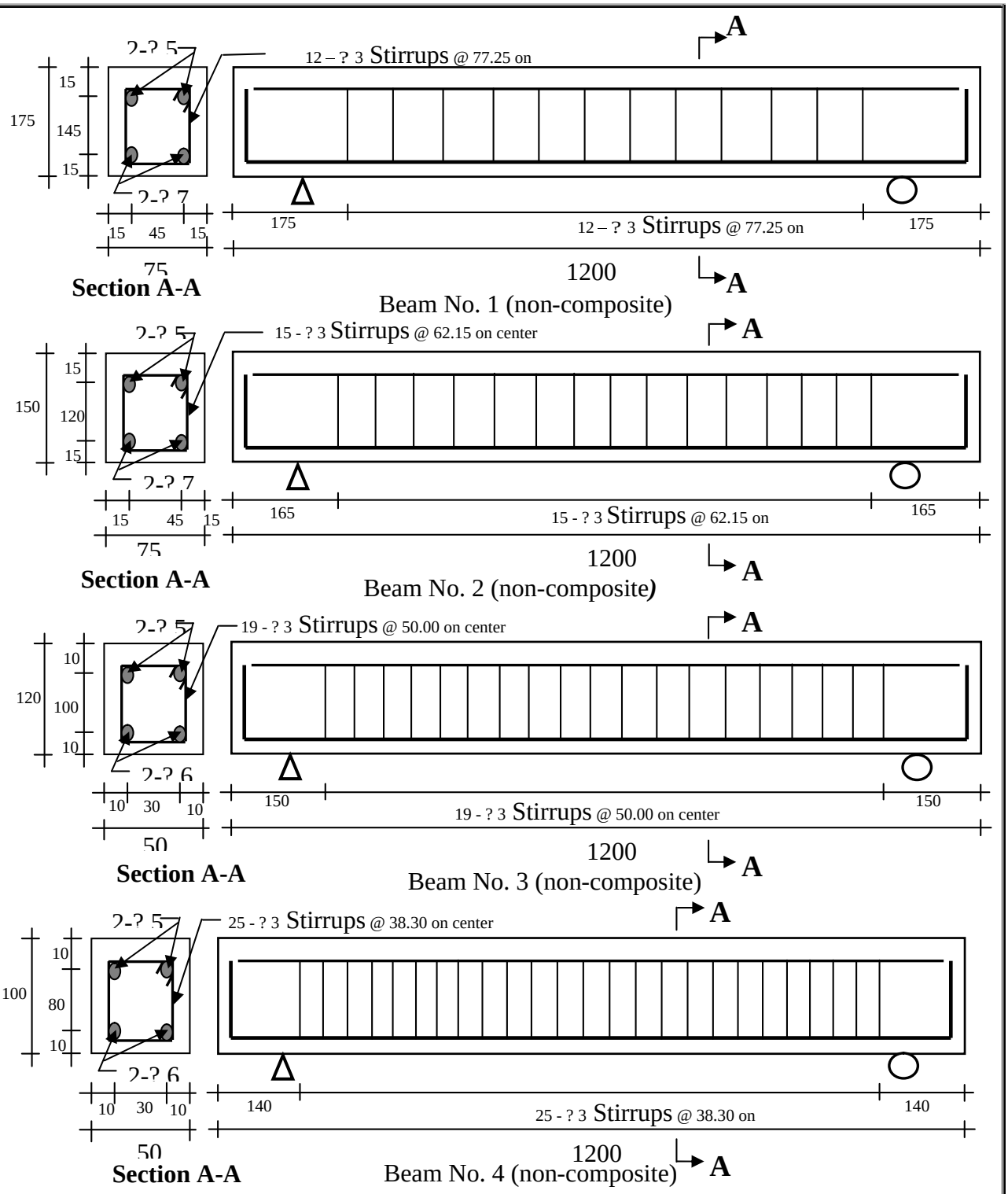

Note: All dimensions are in mm.

Figure (4) Details of the non-composite tested beams

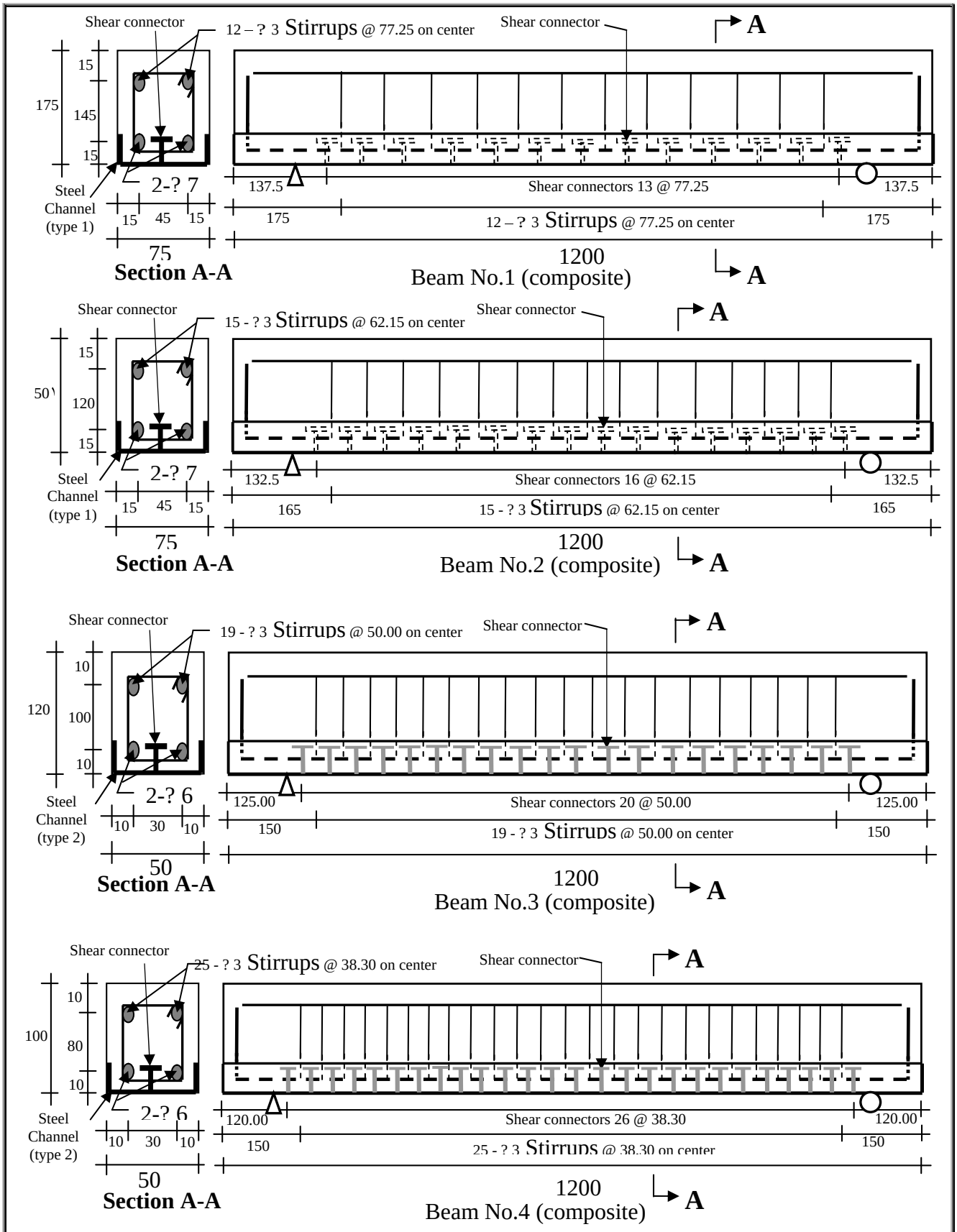

Note: All dimensions are in mm.

Figure (5) Details of the composite tested beams

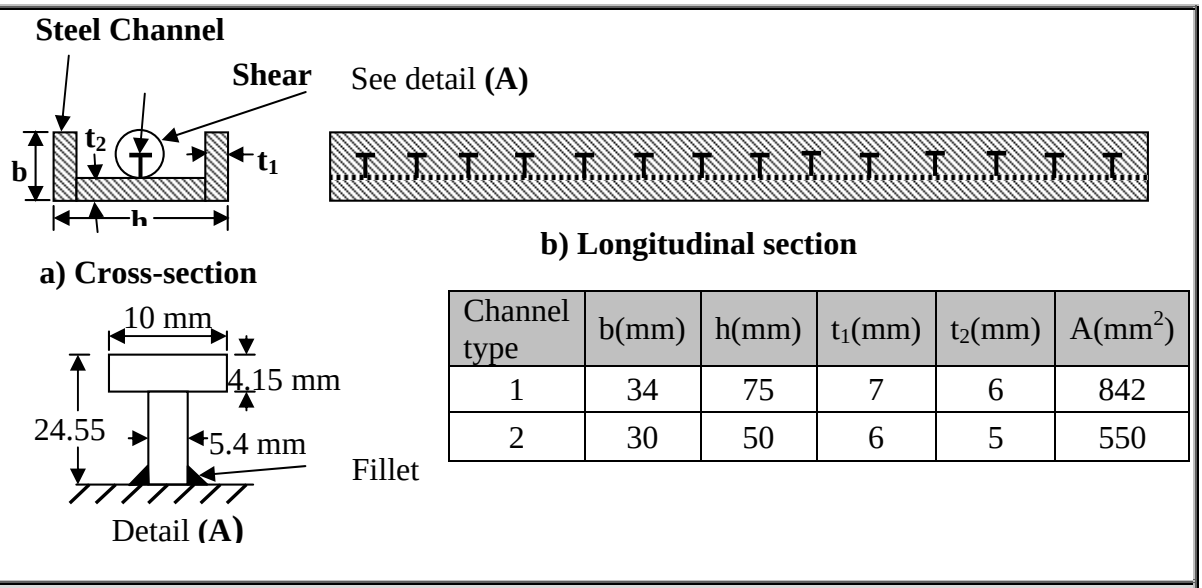

Channel type	b(mm)	h(mm)	t_1(mm)	t_2(mm)	A(mm^2)
1	34	75	7	6	842
2	30	50	6	5	550

Figure (6) Details of the used steel channel and their shear connectors attached by welding

2.2 Materials

Normal weight concrete used in the fabricated beams was produced by mixing sulfate resistant Portland cement, Al-Ukhaider red sand as fine aggregate, and crushed silician gravel of 5 mm maximum size as coarse aggregate. Both the fine and coarse aggregates used in the present work were subjected to sieve analysis according to Iraqi specifications from which the grading curves of Fig. 7 and 8 were drawn showing their locations within the upper and lower limits of these specifications. Mix ratio for concrete constituents was 1:2:4 by weight for cement, sand, and gravel, respectively. Water/cement ratio was 0.4 by weight. The produced concrete mixes were tested for compressive strength using the standard cubes and cylinders of the British standards and the American specifications, respectively.

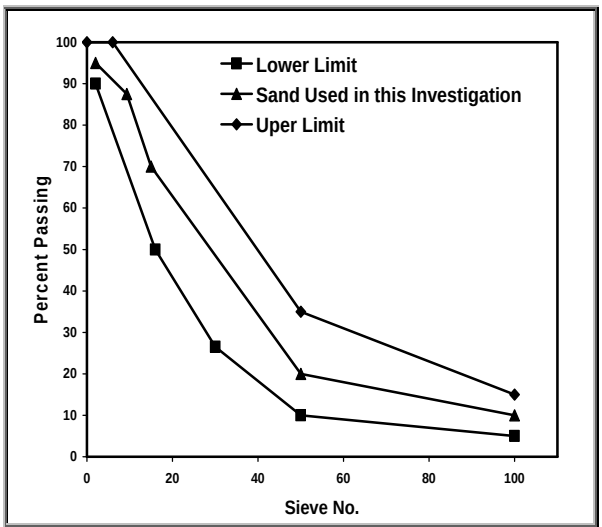

Figure (7) Grading curve of used sand

Results of the compression tests, for three ages, are shown in Table 1. A comprehensive view of the mechanical properties of the produced and cast concrete is given by Table 2.

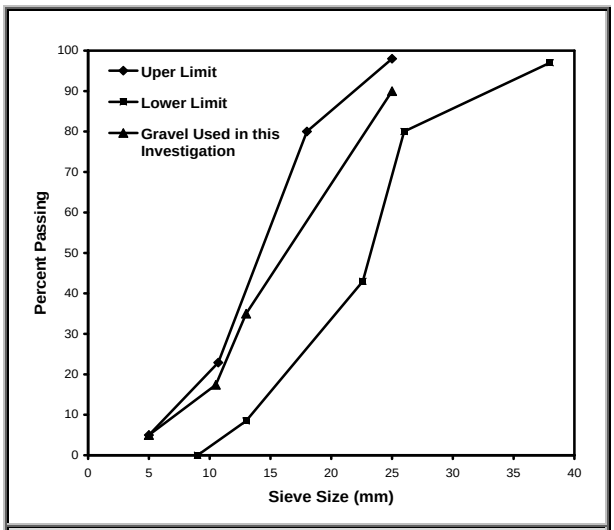

Figure (8) Grading curve of used gravel

With reference to Figs. 4 and 5, four sizes of deformed steel reinforcing bars were used, namely; 3,5,6, and 7 mm in diameter. Tensile tests carried out in the present work on those steel bars gave their mechanical properties presented in Table 3. Young's modulus, yield stress, tensile strength and Poisson's ratio of the structural steel channel were taken from its source as 248 MPa(36 ksi), 400 MPa(58 ksi), 200000 MPa(29000 ksi) and 0.3, respectively. Same values of the specified properties for the steel channel were valid for its shear studs.

Table (1) Results of compression tests according to the British standards (BS) and the American specifications (ASTM) for concrete mixes of the eight test specimens

Age	Compressive strength (MPa)	
	Cylinder**(ASTM)	Cube*(BS)
1 week	17.6	23.9
	13.2	21.9
	16.6	24.0
2 weeks	16.6	31.7
	18.8	31.6
	18.9	31.5
4 weeks	22.7	37.5
	25.8	37.8
	22.7	38.0

*Loading rate=6.8 kN/sec.; BS: British Standards

**Loading rate=5.3 kN/sec.; ASTM: American Society for Testing and Materials

Table(2) Mechanical properties and parameters of the concrete used in fabricating the tested specimens

f_c'	Uniaxial Compression Strength(1)	23.73 MPa
E_c	Young's Modulus(2)	22895.32 MPa
f_t	Tensile Strength(3)	2.44 MPa
ν_c	Poisson's Ratio(4)	0.15
β_0	Shear Transfer Coefficient for Open Crack(4)	0.1
β_c	Shear Transfer Coefficient for Closed Crack(4)	0.99

(1) Cylinder test of the ASTM; average value of the three tests at 28 days age given in Table 1

(2) $E_c=4700\sqrt{f_c'}$

(3) $f_t=0.5\sqrt{f_c'}$

(4) Assumed values

Table (3) Mechanical properties of the steel reinforcing bars used in fabricating the test specimens

E_s	Young's Modulus(*)	207000 MPa
f_y	Yield Stress(*)	412 MPa
f_u	Ultimate Stress(Tensile Strength)(*)	486 MPa

*Obtained from results of tensile tests on the used steel reinforcing bars of the specified diameters (average values).

2.3 Fabrication of Beams and Casting of Concrete

Plate 1-a shows the steel channel part with its shear studs and the side forms which were made of two pieces of 1 mm thick steel plate placed vertically and welded (edge to edge) to the flanges of the steel channel. The fabricated cages of reinforcement were placed at their appropriate positions in the formworks as shown in Plate 1-b. The inside faces of the form were lubricated before placing the reinforcement cages in the proper positions for easy removal of the side forms after hardening of the concrete mix. The concrete mix was then placed in layers and well compacted using vibrating table. Nine cubes were also cast simultaneously for the evaluation of the compressive strength of concrete whose values are shown in Table 1 presented formely. After 24 hours, the formworks were then removed and the beams were submerged in water for 28 days to make the beams ready for test.

a) without reinforcement b) with reinforcement

Plate 1 The steel channel and the steel plate side form welded together for a typical composite tested beam with shear studs welded to interior face of the channel web

2.4 Instrumentation and Testing Procedure

The eight specified beam specimens were tested in the Civil Engineering Laboratory of Nahrain University using the electrical loading machine (shown in plate 2) provided by a calibrated load cell of 0.01 mm accuracy for load measurement. With reference to Fig. 9, one point load located at mid-span was applied for each beam at a constant rate by the loading machine with one dial gauge of 0.01 mm precision placed at the beam soffit directly beneath the load. The dial gauge readings were recorded at 5 kN load increments. This procedure continued until failure of the tested specimen was reached. Locations, orientation, widths, and propagations of all cracks along each beam span were marked and recorded during the loading procedure.

Plate 2 Testing machine and beam specimen

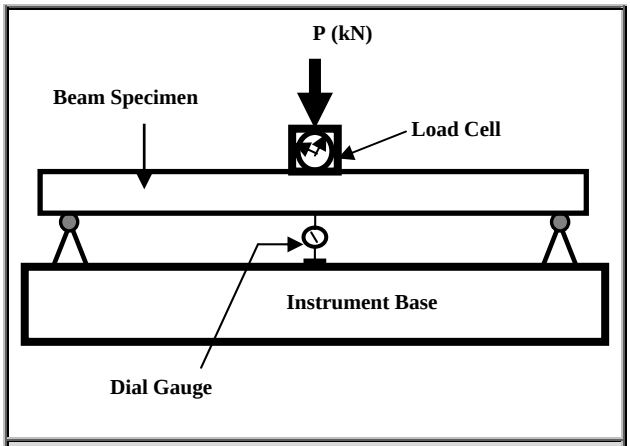

Figure (9) Schematic diagram for test arrangement

4. Finite element modeling

4.1 Definition

The commercial finite element analysis package ANSYS [6] (Analysis System Version 5.4) was set up (with its parameters calibrated) and used in the analysis of the present four composite beams (comprising integrated steel channels) and the four associated non-composite ones. The program has the capacity of solving linear and nonlinear problems including the effects of nonlinearity properties of materials and contact surfaces, and shear and split interaction at the contact surfaces of the concrete and the integrated steel channel. From the 165 different elements included in the program, three element types are selected to model the composite and the non-composite beams of the present study as given later on.

Material Nonlinearities The nonlinearity properties taken into account through ANSYS operations in modeling the present composite and non-composite beams are concrete cracking and crushing in tension and compression respectively, yielding of the steel reinforcing bars and the structural steel channel, and the slip at interfaces between reinforced concrete and the steel channel.

Element Types

1-Reinforced concrete

The 8-node isoparametric linear brick elements SOLID65 with three translational degrees of freedom at each node shown in Fig.10 is used in the present work for modeling the reinforced concrete. This element is capable of plastic deformation, cracking in three orthogonal directions, and crushing.

2-Steel reinforcing bars

Steel reinforcement (including longitudinal bars and transverse stirrups) are introduced into the brick SOLID65 element by assuming it smeared throughout the element. Any orientation of the steel rebars is permitted. Use of this approach is supported by the fine mesh of concrete media, especially at rebar locations as recommended by the program [6].

3-Structural steel channel

The 4-node isoparametric linear flat shell element SHELL63 of both bending and membrane capabilities and with three translational and two rotational degrees of freedom at each node shown in Fig.11 is used for modeling the steel channel. Stress stiffening and larger deflection capabilities are included

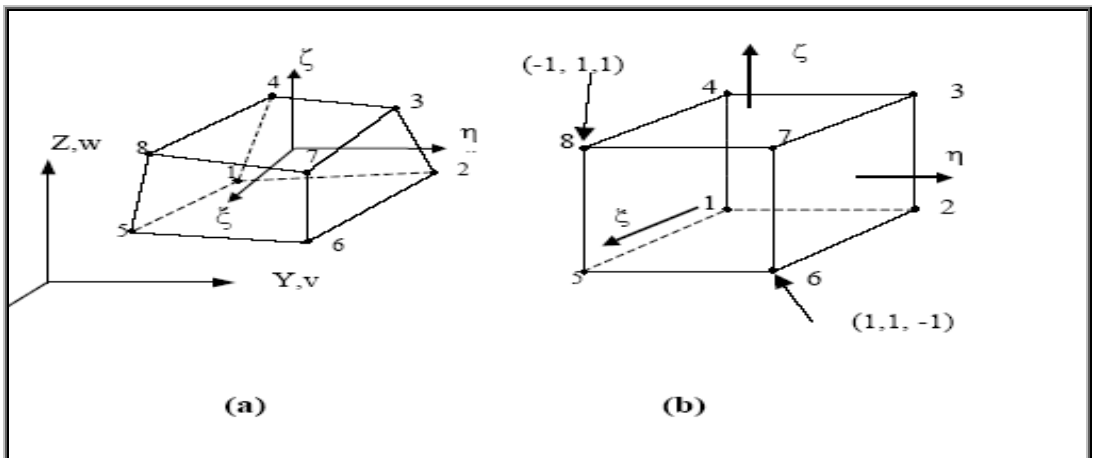

Figure (10) The 8- node brick element SOLID65 used for modeling reinforced concrete:
(a) global coordinate system
(b) local coordinate system [6]

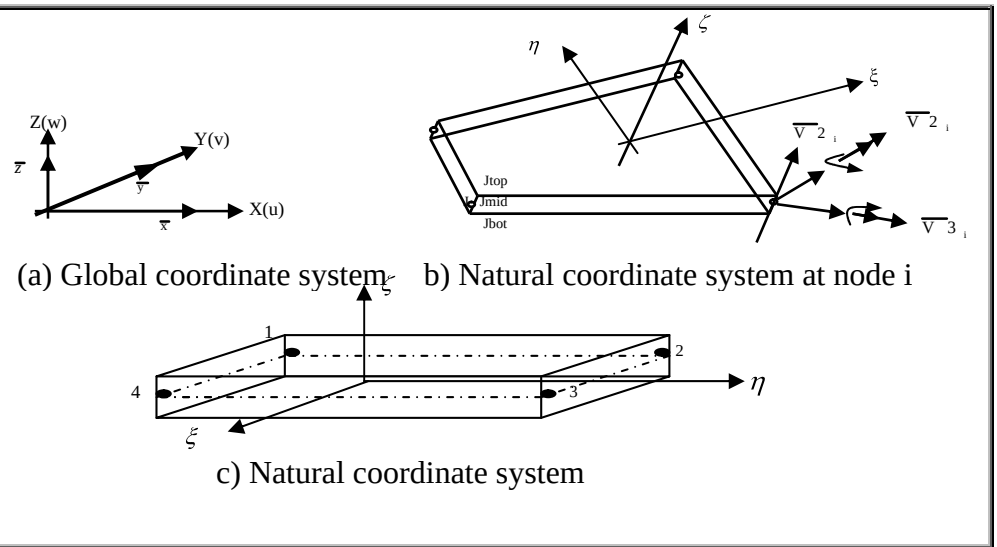

(a) Global coordinate system b) Natural coordinate system at node i

c) Natural coordinate system

Figure (11) Four-node isoparametric flat shell element SHELL63 used for modeling the steel channel [6]

4-Interface between concrete and steel channel

The 5-node interface finite element CONTACT49 with three translational degrees of freedom at each node shown in Fig.12 is used for modeling the contact and the sliding at the contact surfaces of concrete and the steel channel.

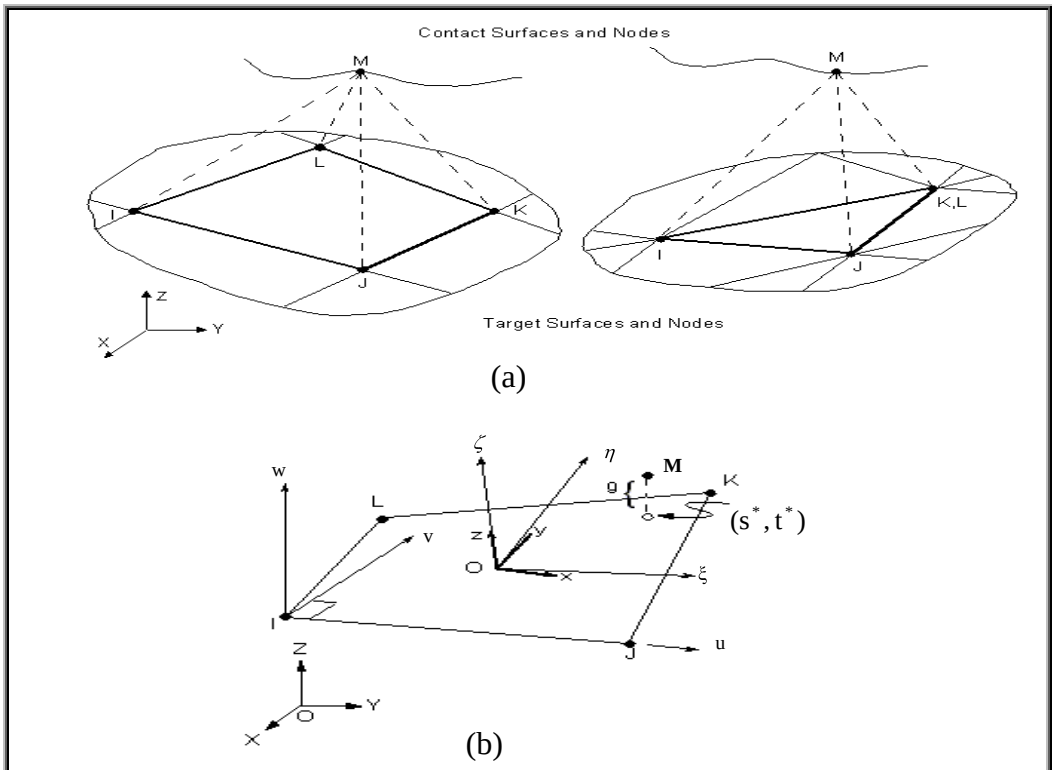

Figure (12) The three-dimensional node-to-surface interface elements CONTACT49[6]:
(a) Geometry (b) Natural coordinate system

Meshing

Meshes of the reinforced concrete media in the present eight composite and non-composite beams are generated to consist of cubic elements (or ones of rectangular faces if the cubic discretization is impossible) as recommended by the package[6].

Loads and boundary conditions

To avoid crushing of the concrete under the effects of concentrated external loads and supports reactions, the mid-span applied loads and the end reactions are replaced by equivalent force systems of identical nodal forces at locations of the external forces and the reactions in their vicinities as shown in Figs. 13 and 14 given later on.

Nonlinear solution algorithm

The nonlinear equations of equilibrium are solved using an incremental iterative technique under load procedure. The full Newton-Raphson method is used for the nonlinear solution algorithm and the displacement criterion is used as a convergence criterion [6], with a convergence tolerance of 5%.

Numerical integration

Eight-point (2x2x2) integration rule for the reinforced concrete brick elements and four-point (2x2) integration rule for the steel channel section elements and for the interface elements are used for numerical integration.

APPLICATIONS

Scheme

The present applications include primarily analysis of results drawn from loading tests (described in the previous section) of the eight fabricated beams classified in two groups (composite and associated non-composite ones). They also include finite-element modeling by ANSYS-package for those beams and analysis of results predicted by it.

The primary object of the applications is to determine the load-deflection relation for each beam experimentally and by the finite element method, so that a first comparison between them is made to assess accuracy of the suggested finite element model. A second comparison between behaviors of the composite beams and their associated non-composite ones is also made to evaluate the effect of the composite action represented by introducing the integrated steel channel.

A further object of those applications is to *bring out* the cracking patterns drawn from the experimental work and those predicted by the finite element models for each of the eight beams and making comparisons by the same procedure used for the primary object.

Studied parameters

i.stiffness at the linear and the post-cracking stages
ii.ultimate load capacity
iii.deflection at ultimate stage

note: i,ii,iii extracted from load-deflection relation for each beam.

iv. mode of failure – deduced from the cracking pattern at ultimate stage for each beam.

ANSYS models for the experimental beams

The finite element meshes, boundary conditions, and loading arrangements by ANSYS program using the three previously defined ANSYS finite elements to model reinforced concrete, steel channel, and shear studs for each of the four specified composite beams and the four associated non-composite ones are shown in Fig.13 and 14, respectively. These two figures also show the cross-section-wize element division where it can be noticed that SOLID65 elements representing reinforced concrete media are divided into five and four sets for the composite and the associated non-composite beams, respectively. Each set has different parameters (real constants) depending on amounts of the longitudinal and the transverse reinforcing bars in its elements. Detailed information concerning total numbers of nodes, SOLID65 brick element, SHELL63 flat shell elements, and CONTACT49 interface elements are given in Table 4 below for each of the eight specified composite and non-composite beam

PRESENTATION AND DISSCUSION OF RESULTS

Characteristics of Flexural Behavior

a) Comparison between test and numerical results (with reference to Fig. 15):

In general, close agreements between the load-deflection behaviors given by the laboratory loading tests and those predicted by the present finite element models by ANSYS program for the four composite beams and the four associated non-composite ones, thus verifying the accuracy and efficiency of the present numerical modeling. However, while the highly-accurate finite element models for the four composite beams produced a margin of discrepancy with the test specimens not exceeding 11 % (for deflection) in the absolutely worst case, finite element models for the four associated non-composite beams (recorded further higher accuracy in comparison with results of the test specimens). The absolute maximum difference in deflection values of this case does not exceed 7%. This may be attributed to the finite element modeling of shear connector by interface elements.

b) Variation in the main flexural parameters with introducing the integrated steel channel (with reference to Table 5):

i) The ultimate load capacity increases with introducing the integrated steel channel. That increase depends mainly on increase of the ratio of "**steel channel cross-sectional area/gross area of cross-section**". The minimum value of the increase percentage in that parameter is **155%** for **Beam 1** where $\mathbf{A_{ch}/\ A_g}$ **=0.064** while the maximum increase percentage value is **500%** for **Beam 4** where $\mathbf{A_{ch}/\ A_g}$ **=0.11**. These huge increase percentage values of ultimate loads indicate *the tremendous effect of introducing the integrated steel channel on ultimate load capacity*.

ii) The mid-span deflection at ultimate stage decreases with introducing the integrated steel channel. That decrease depends mainly on the increase of the ratio of "**steel channel cross-sectional area/bottom reinforcement cross-sectional area**". In this respect the four beams are divided into two groups, **the first group (comprising beams 1 and 2)** undergoes **large** values of decrease percentage (definitely between **25.5% and 27%**) owing to their **high** values of $\mathbf{A_{ch}/\ A_{s(bott.)}}$ ratio value**(10.94)**. The second group **(comprising beams 3 and 4)** suffers lower values of decrease percentage (**15.64% average value)** due to their low value of $\mathbf{A_{ch}/\ A_{s(bott.)}}$ ratio **(9.72)**. Value of $\mathbf{A_{ch}/\ A_g}$ ratio has *no* distinct positive effect on that parameter as may initially be expected.

iii) The initial flexural stiffness increases with introducing the integrated steel channel. That increase depends solely on the **increase** in the value of "$\mathbf{A_{ch}/\ A_g}$" ratio, where **rather rapid increases** in that flexural parameter occur with **monotonic increases** in $\mathbf{A_{ch}/\ A_g}$ ratio.

Table (4) Numbers of nodes, brick elements, flat shell elements, and interface elements for each of the eight specified beams

		Total No, of Nodes	Total No, of SOLID65 elements	Total No, of SHELL63 elements	Total No, of CONTACT49 elements	Total No, of elements
Composite beam	CB*-1	352	135	75	75	285
	CB*-2	418	162	90	90	342
	CB*-3	391	132	88	88	308
	CB*-4	493	168	112	112	392
Non-composite beam	NCB**-1	256	135	-	-	135
	NCB**-2	304	162	-	-	162
	NCB**-3	276	132	-	-	132
	NCB**-4	348	168	-	-	168

* CB symbol denotes to composite beam.
** NCB symbol denotes to non-composite beam.

Table (5) Variations of ultimate load capacities, mid span deflections at ultimate stages, and initial flexural stiffnesses for beams 1, 2, 3, and 4 with introducing the integrated steel channels

Beam No.	$\mathbf{A_{s(bott.)}/\ A_g}$	$\mathbf{A_{ch}/\ A_g}$	$\mathbf{A_{ch}/\ A_{s(bott.)}}$	Percentage of variation due to introducing the integrated steel channel*		
				Ultimate Load Capacity ▲	Mid-span Deflection at Ultimate Stage ▲	Initial Flexural Stiffness ▲
Beams 1	0.0059	0.064	10.94	+155%	–27%	+15.8%
Beams 2	0.0068	0.075	10. 94	+178%	–25.5%	+18.3%
Beams 3	0.0094	0.092	9.72	+275%	–20%	>+200%
Beams 4	0.0113	0.11	9.72	+500%	–10.64%	>+200%

* From load-deflection curves shown in Fig. 15.
▲+ve and –ve signs refer to increase and decrease, respectively.

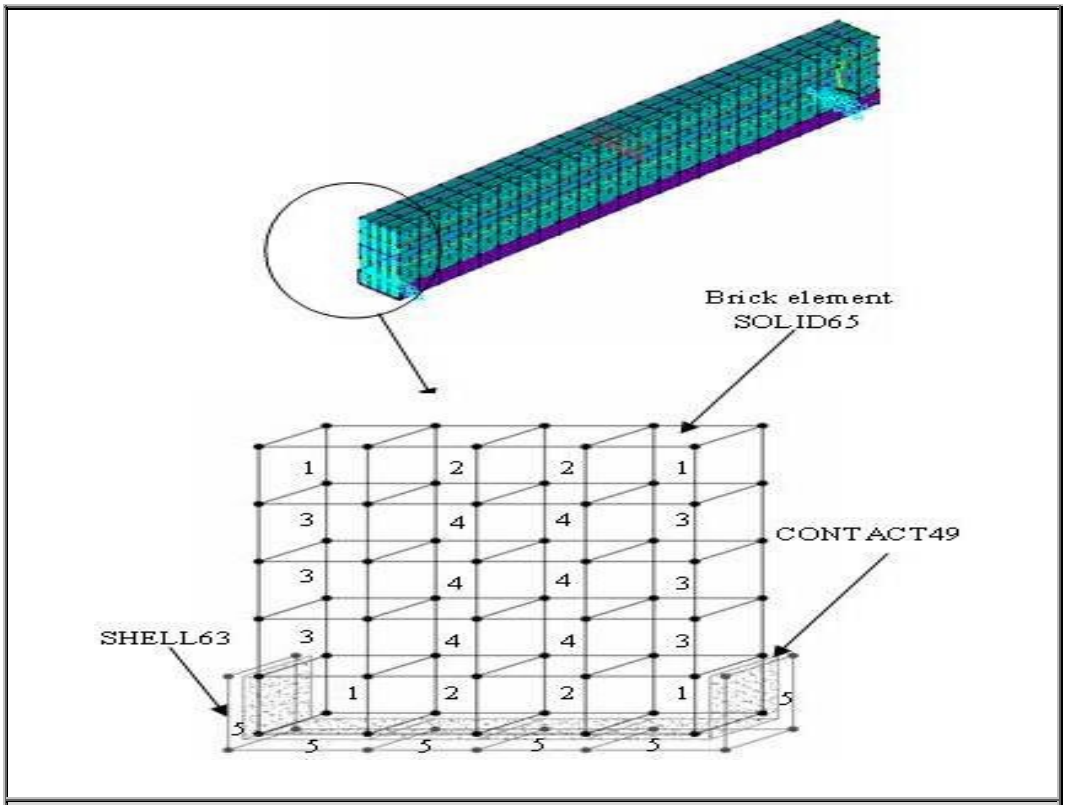

Figure (13) Finite element meshing, boundary conditions, and loading arrangement by ANSYS model for each of the four specified composite beams

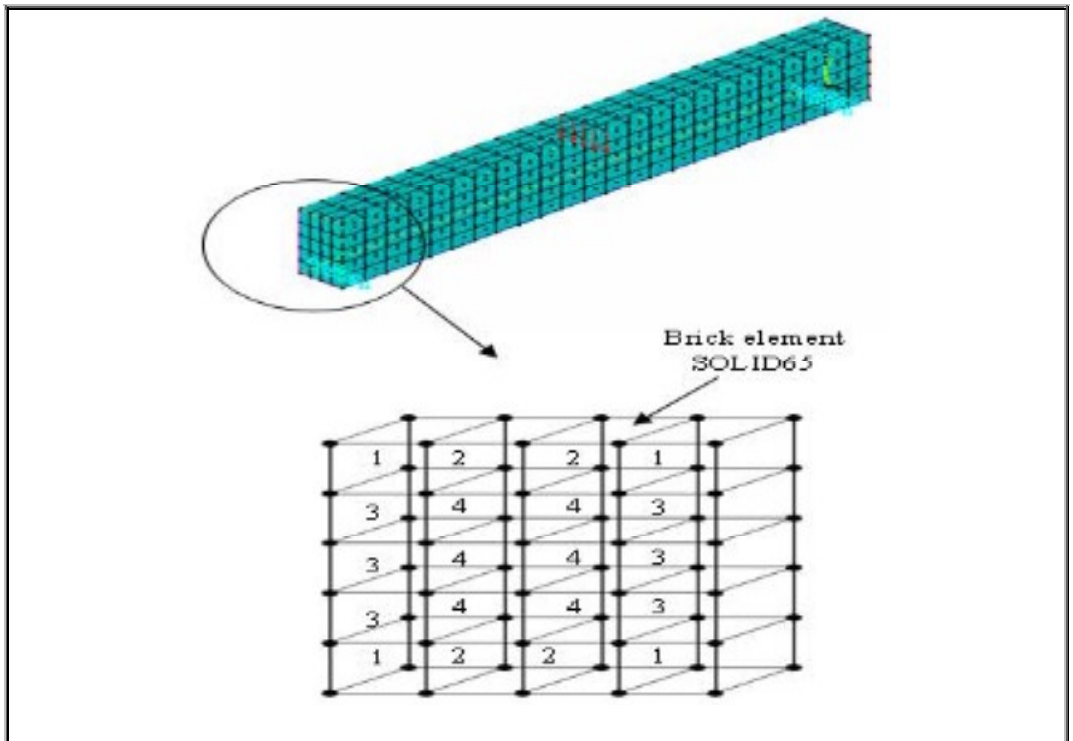

Figure (14) Finite element meshing, boundary conditions, and loading arrangement by ANSYS model for each of the four specified non-composite beams

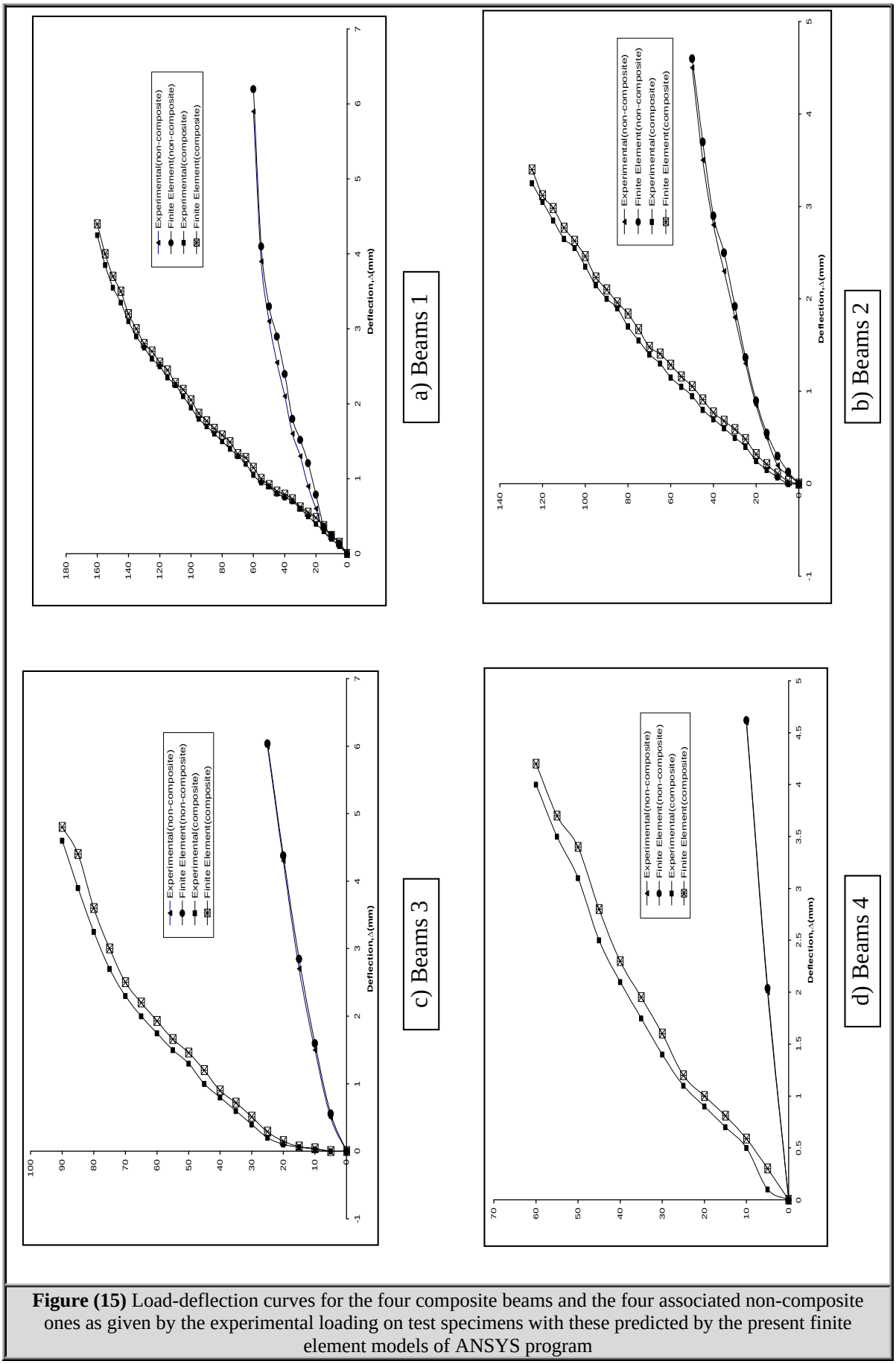

Figure (15) Load-deflection curves for the four composite beams and the four associated non-composite ones as given by the experimental loading on test specimens with these predicted by the present finite element models of ANSYS program

Modes of Failure

The fracture patterns at ultimate stages (resulting from the monotonic loading tests for the four fabricated composite (except beam 1) and four non-composite specimens beams) are shown in Plates 3 and 4, respectively. While the mode of failure for the typical composite beam resulting from experimental work is **a crushing mode of concrete in the compression zone at the middle one-fifth of the simple span**, the typical mode of failure for the non-composite beams (given by loading tests) is an **excessive concrete tension cracking mode converging the top surface and accompanied by yielding of the bottom steel reinforcing bars**.

With reference to Figs. 16 and 17, the present numerical models by ANSYS program for the four composite beams and the four non-composite ones predict the fracture patterns for each of the two types of beams within three consecutive loading stages; 30%, 60%, and 100% of ultimate loads. They also predict the modes of failure for the two cases (composite and non-composite ones). It is noticed that these modes of fracture coincide with the corresponding ones given by the experimental work.

Plate (3) Typical composite beam at failure (crushing of concrete in compression zone at the middle one-fifth of the simple span)

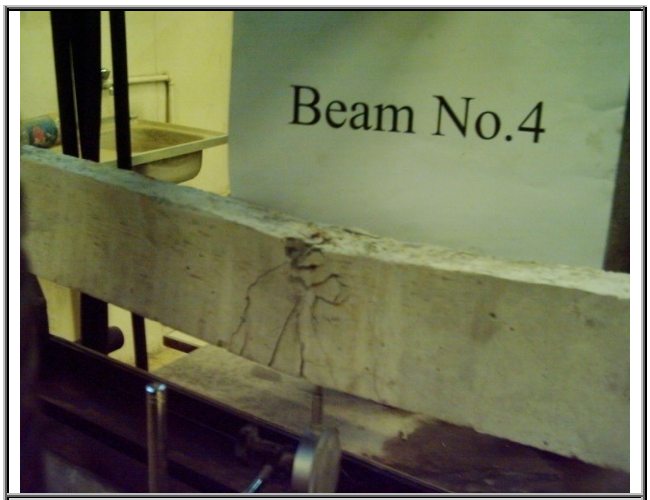

Plate (4) Typical non-composite beam at failure (yield of bottom steel reinforcing bars with excessive tension cracks converging the top surface)

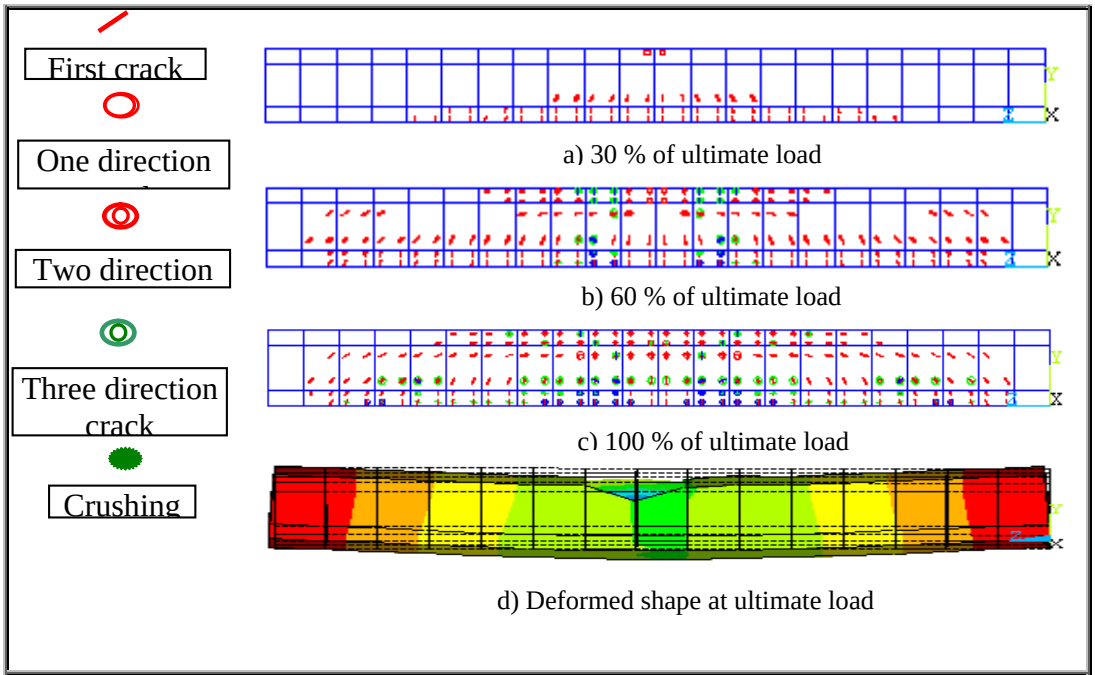

Figure (16) Fracture patterns for the typical composite beam within consecutive loading stages showing mode of failure due to crushing of concrete in the compression zone at the middle one-fifth of the simple span

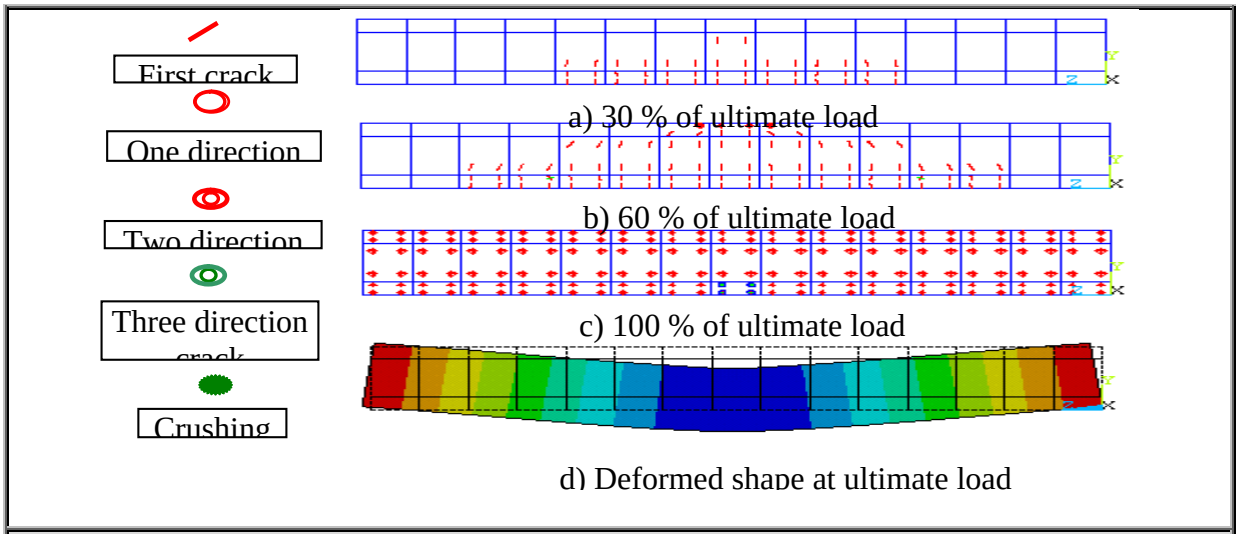

Figure (17) Fracture patterns for the typical non-composite beam within consecutive loading stages showing mode of failure due to excessive tension cracks converging the top surface and accompanied by yield of bottom steel reinforcing bars

PRAMETRIC STUDY

Effect of Introducing The Integrated Steel Channel on Beam Ductilit

With reference to Table 6 (which gives a comprehensive view on values of the ductility ratio for the present eight composite and non-composite beams) the following remarks specifying parameters affecting ductility ratio can be regarded:

i) Values of the ductility ratio for the non-composite beams **decrease** with the **increase** of $\mathbf{A_{s(bott.)}/ A_g}$ **ratio**. As the latter ratio **increases** from **0.0059** for non-composite **beam 1** to **0.0113** for non-composite **beam 4** the ductility ratio decreases from **1.69** to **1.29**.

ii) Values of the ductility ratio decrease with introducing the integrated steel channel. That decrease depends mainly on the $\mathbf{A_{ch}/ A_{s(bott.)}}$ **ratio**. In this respect the four beams are divided into two groups. **The first group** (comprising beams 1 and 2) undergoes large values of decrease percentage (definitely between **36.7%** and **36.9%**) owing to their **high** value of $\mathbf{A_{ch}/ A_{s(bott.)}}$ ratio (**10.94**). **The second group** (comprising beams 3 and 4) suffers lower values of decrease percentage (between **26.4%** and **27.3%**) due to their low value of $\mathbf{A_{ch}/ A_{s(bott.)}}$ ratio (**9.72**). Value of $\mathbf{A_{ch}/ A_g}$ ratio has no regular effect on ductility ratio.

iii) Decrease of ductility ratio due to introducing integrated steel channels can be kept within acceptable limits by **reducing values of** $\mathbf{A_{s(bott.)}/ A_g}$ **ratio** relatively to the extent giving **ductility ratio≥1.0** even with using steel channel. Referring to Table 6, this is the case of **the composite beam 1**.

Table (6) Variation of values of the ductility ratio for beams 1, 2, 3, and 4 with steel reinforcing bars ratios and with introducing integrated steel channels

		$A_{s(bott.)}/ A_g$	A_{ch}/ A_g	$A_{ch}/ A_{s(bott.)}$	Mid-span Deflection At 1st yield Δ_y (mm)*	Mid-span Deflection At Ultimate Stage Δ_u (mm)*	Ductility ratio Δ_u / Δ_y	% of decrease in ductility ratio due to introducing the steel channel
Beams 1	Non-composite	0.0059	—	—	3.72	6.3	1.69	36.7%
	composite	—	0.064	10.94	4.3	4.6	1.07	
Beams 2	Non-composite	0.0068	—	—	2.99	4.7	1.57	36.9%
	composite	—	0.075	10.94	3.54	3.5	0.990	
Beams 3	Non-composite	0.0094	—	—	4.41	6.0	1.36	27.3%
	composite	—	0.092	9.72	4.85	4.8	0.989	
Beams 4	Non-composite	0.0113	0	—	3.64	4.7	1.29	26.4%
	composite	—	0.11	9.72	4.42	4.2	0.950	

* Computed by the present finite element models of ANSYS program

Effect of Flange Widths; b_f of the Integrated Steel Channels on Flexural Behavior of Composite Beams

With reference to Fig. 18 which shows the load-deflection curves of the composite beam 1 for three values of flange width; $\mathbf{b_f}$ of the integrated steel channel(definitely the original width 34 mm, 40 mm, and 45 mm), it can be noticed that this factor has a significant effect on flexural properties and parameters of the composite beam.

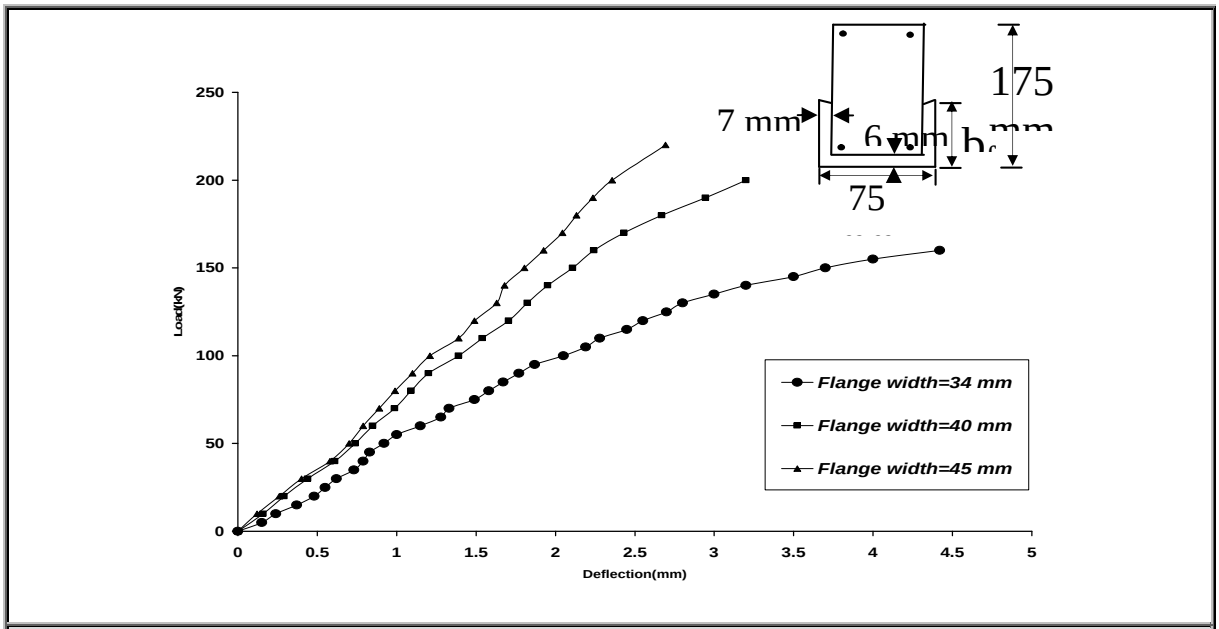

Figure (18) Load-deflection curves of composite beam 1 for different values of flange width; $\mathbf{b_f}$ of the integrated steel channel

Table (7) Variations in values of the main flexural properties and parameters of the composite beam 1 with increasing flange width of the integrated steel channel

Flange width; $\mathbf{b_f}$ (mm)	Mid-span Deflection At 1st yield Δ_y (mm) **	Mid-span Deflection At Ultimate Stage Δ_u (mm) **	Ductility ratio Δ_u / Δ_y	Percentage of variation due to increasing flange width of the integrated steel channel(relative to b_f =34 mm)*			
				Ductility ratio	Ultimate load capacity ▲	Mid-span deflection at ultimate stage ▲	Flexural stiffness at linear stage ▲
34	4.3	4.6	1.07	0	0	0	0
40	4.26	4.3	1.01	– 5.5%	+ 25%	– 27%	+34%
45	4.2	4.2	1.00	– 6.1%	+37%	– 39%	+38

* +ve and –ve signs refer to increase and decrease, respectively.
** computed by the present finite element models of ANSYS program
▲ from load-deflection curves shown in Fig. 18

Variation of values of main four flexural parameters with various values of the flange width are all given numerically in Table 7, and can be discussed as follows:

a) Ductility ratio decreases with increase of b_f. **As** b_f increases to 40 mm and 45 mm, the ductility ratio decreases by 5.5% and 6.1%, respectively. Those values of decreases are small and do not lower the ductility behavior significantly.

b) Ultimate load capacity increases with increase of $\mathbf{b_f}$. As $\mathbf{b_f}$ increases to 40 mm and 45 mm, the ultimate load capacity increases by 25% and 37%, respectively. Such increases are large enough to increase $\mathbf{b_f}$ as far as possible.

c) Mid-span deflection at ultimate stage decreases (by large percentage reaching 39% in one studied case) with the increase of $\mathbf{b_f}$, a property leading to benefit from increasing $\mathbf{b_f}$ in using such composite beams in large span floor systems and trusses.

Flexural stiffness at linear stage increases rapidly with increase of $\mathbf{b_f}$**.** Percentage increase in that stiffness reaches 38% for a 11 mm increase in $\mathbf{b_f}$. The same above benefit may be applied based on that fact.

CONCLUSIONS

1. A study of the tests reported herein shows that use of integrated steel channels at soffits of rectangular cross-section reinforced concrete beams is quite beneficial for design purposes, since it extremely improves the ultimate load capacity criterion. The sevisiblity criteria (extent of cracking, excessive deflection, and low flexural stiffness) are considerably improved.
2. The unique drawback against wide use of this type of composite beams is the lowering of their ductility due to introducing the integrated steel channels. However, that unfavorable impression can be removed by reducing the tensile reinforcement ratio by the amount sufficient for removal of that effect, to keep the composite beam (finally) far from any crushing of compression concrete at failure.
3. The present finite element treatment of the specified composite beams and their associated non-composite ones by ANSYS package (based on modeling the reinforced concrete by eight-node brick elements, the steel channel by four-node shell elements, and the five-node interface elements at the contact surface) produced high agreement with the present experimental test results. While the finite element model of the composite beams gives maximum discrepancy from the test results (for deflections) not exceeding 11%, the finite element model of the non-composite beams gives rather higher accuracy represented by maximum difference from test results not exceeding 7%.
4. The fracture pattern at ultimate stage predicted by the present finite element models (for the composite and the non-composite beams) are identical to those resulting from the present load test on the fabricated specimens. A crushing failure mode of concrete in the compression zone at the middle one-fifth of the simple span is obtained for each composite beam (except beam 1) , and an excessive tensile concrete cracking mode converging the top surface with accompanying yield of the bottom steel reinforcing bars is produced for the non-composite beams.
5. The increase in ultimate load capacity (due to introducing integrated steel channels) depends mainly of the $\mathbf{A_{ch}}$/ $\mathbf{A_g}$ ratio. The higher the value of the former ratio, the higher is the increase percentage in ultimate load capacity. That increase percentage is within the 155% to 500% limits for the four pairs of tested beams.
6. The decrease of mid-span deflection at ultimate stage (with introducing the integrated steel channels) depends on the $\mathbf{A_{ch}}$/ $\mathbf{A_{s(bott.)}}$ ratio. The higher the former ratio the higher is the decrease in deflection value.
7. As for the deflection at ultimate stage (the previous term), the amount of reduction in ductility ratio values (with introducing the integrated steel channels) depends on the $\mathbf{A_{ch}}$/ $\mathbf{A_{s(bott.)}}$ value with a similar trend of variation.
8. The increase of flange width of the integrated steel channel has a considerable effect on the ultimate load capacity of the composite beam where a 37% increase in that capacity is achieved with 11 mm increase in the flange width of the composite beam 1. Meanwhile an inefficient decrease of 6.1% in the ductility ratio occurs. That practice urges the designers towards introducing steel channels of large flange width.

NOTATION

$\mathbf{A_{ch}}$	Cross-sectional area of the integrated steel section
$\mathbf{A_g}$	Cross concrete area of beam cross-section
$\mathbf{A_{s(bott.)}}$	Cross-sectional area of bottom steel reinforcing bars
$\mathbf{E_c}$	Modulus of Elasticity of concrete
$\mathbf{E_s}$	Modulus of Elasticity of Steel Structural Channel and reinforcing bars
$\mathbf{f'_c}$	Uniaxial compressive strength of concrete (cylinder test)
$\mathbf{f_t}$	Uniaxial tensile strength of concrete
$\mathbf{F_y}$	Yield stress of the structural steel channel (AISC-specification)
$\mathbf{f_y}$	Yield stress of the steel reinforcing bars (ACI-code)
u, v, w	Displacement components in x, y and z directions, respectively
X,Y,Z	Global coordinate system
x, y, z	Cartesian coordinates
Δ_y	Beam mid-span deflection at first yield of steel channel or bottom reinforcing bar
Δ_u	Beam mid-span deflection at ultimate stage
β_o, β_c	Shear transfer coefficients for open and closed cracks, respectively

ν	Poisson's ratio
ξ, η, ς	Local coordinates

REFERENCE

1. Taylor,R., "Composite Reinforced Concrete", Thomas Telford Limited,London.1979.
2. Taylor,R. and Burdon ,P., "Tests on a New Form of Composite Construction", Proceedings of the Institution of Civil Engineers, Part 2:Research and Theory, Vol.47, September, 1970, pp. 43-54.
3. Taylor,R. and Najmi A.Q.S., "Composite Reinforced Concrete Beams in Hogging Bending", Proceedings of the Institution of Civil Engineers, Part 2:Research and Theory, Vol.69, September, 1980, pp. 801-812.
4. Yousif,M., "Flextural Behavior of Composite Reinforced Concrete Beams ", M.Sc. Thesis, Basrah University ,Basrah, Iraq, 1982.
5. Abd Al-Razag,N., "Flextural Behavior of Composite Reinforced Concrete Beams ", M.Sc. Thesis, Basrah University ,Basrah, Iraq, 1985.
6. ANSYS Manual, Version 5.4, 1997.
7. Chen, W. F., "Plasticity in Reinforced Concrete", McGraw-Hill Book Company, Inc., New York, 1981.

دراسة عملية وبطريقة العناصر المحددة للروافد المركبة المكونة من عتبات خرسانية مسلحة مصبوبة في حديد الساقية

د.ليث خالد الحديثي
مدرس
جامعة النهرين/كلية الهندسة
E-mail:lthadithy@yahoo.com

عمر خالد الكربولي
ماجستير في الهندسة الانشائية
E-mail:omerkhalid79@yahoo.com

الخلاصة

تم في الدراسة الحالية التصنيع والتحميل والفحص المختبري لأربعة روافد خرسانية مسلحة ذوات مقاطع عرضية مستطيلة ، واربعة روافد مركبة مقابلة لها تتكون من عتبة (موشور prim) خرسانية مسلحة مصبوبة في قطعة حديد ساقية مع روابط قص ، وذلك لغرض قياس الهطول في منتصف الفضاءات ولمعاينة ظاهرة التصدع.ان الموشور prism الخرساني المسلح لكل من الروافد المركبة الأربعة ذو مقطع عرضي مستطيل مماثل للمقطع العرضي للرافدة الخرسانية المسلحة (غير المركبة) المقابلة لها.

كما تمت مقارنة سلوك الحمل-الانحراف ونمط التصدع عند الفشل المستحصلين من الفحص المختبري لتلك الروافد (المركبة وغير المركبة) مع السلوك المحسوب من قبل التحليل اللاخطي ثلاثي الأبعاد بالعناصر المحددة باستخدام برنامج التحليلات الأنشائية ANSYS V. 5.4 الذي تم فيه تمثيل الخرسانة المسلحة ، حديد الساقية ، والترابط بين الخرسانة المسلحة ومقطع حديد الساقية بالعناصر الطابوقية ذوات الثمان عقد ، العناصر القشرية ذوات الأربع عقد ، والعناصر البينية خماسية العقد ، على التوالي.

تم الحصول على توافق عال بين نتائج الفحوصات المختبرية والنماذج الرياضية في سلوك الحمل-الأنحراف والذي يتمثل في قيم قصوى للأختلاف لاتتجاوز نسب ١١% و٧% للروافد المركبة وغير المركبة ، على التوالي.علاوة على ذلك ، فقد تحقق التطابق التام بين الطريقتين في تحديد نمط التصدع عند الفشل.

ان المقارنات بين سلوك الأنحناء - لكل زوج من الازواج الاربعة الحالية للروافد المتقابلة المركبة وغير المركبة - تبين بأن استحداث حديد الساقية المدمج يرفع قيم قابلية التحمل القصوى بنسب تتراوح بين ١٥٥% و ٥٠٠% - أعتمادا على نسبة مساحة مقطع حديد الساقية الى مساحة المقطع الخرساني الاجمالي ، مع خفض نسب المطيلية بنسب تتراوح بين ٢٦.٤% و ٣٦.٧% - أعتمادا على مساحة مقطع حديد الساقية الى مساحة مقطع حديد تسليح الشد.

بينت دراسة مقارنة بخصوص تأثير عرض طوق مقطع حديد الساقية بأن زيادة قدرها ٤٠% في قابلية التحمل القصوى يمكن تحقيقها بزيادة عرض طوق مقطع حديد الساقية بمقدار الثلث ، يرافقها نقصان طفيف في نسبة المطيلية.